Accepted manuscript

Regional fat mass estimation using bioelectrical impedance analysis in healthy adults

Analiza M. Silva[1*], Tiago R. Silva[1,2], Pedro B Júdice[3,4], Gil B. Rosa[1], Ana V. Bernardino[1], João P. Magalhães[1], Inês R. Correia[1], Megan Hetherington-Rauth[5], Luís B. Sardinha[1]

[1]Exercise and Health Laboratory, CIPER, Faculdade Motricidade Humana, Universidade Lisboa, Estrada da Costa, 1499-002 Cruz-Quebrada, Portugal;
[2]Faculty of Nutrition and Food Sciences, University of Porto, Rua do Campo Alegre, 823, 4150-180 Porto, Portugal
[3]Centro de Investigação em Desporto, Educação Física, Exercício e Saúde (CIDEFES), Universidade Lusófona, Lisboa, Portugal.
[4]Centro de Formação, Inovação e Intervenção em Desporto (CIFI2D), Porto, Portugal.
[5]California Pacific Medical Center, Research Institute, San Francisco, CA, USA

Corresponding Author:** ***Analiza Mónica Silva, Ph.D. Exercise and Health Laboratory, CIPER, Faculdade de Motricidade Humana, Universidade de Lisboa; Estrada da Costa, 1499-002 Cruz-Quebrada Portugal Telephone: + 351 21 4149172 | Email: analiza@fmh.ulisboa.pt

Short title: BIA-based regional fat mass models

This peer-reviewed article has been accepted for publication but not yet copyedited or typeset, and so may be subject to change during the production process. The article is considered published and may be cited using its DOI
10.1017/S0007114525000510
The British Journal of Nutrition is published by Cambridge University Press on behalf of The Nutrition Society

ABSTRACT

Whole-body and regional raw bioelectrical impedance analysis (BIA) parameters have been used to develop lean soft tissue estimation prediction models. Still, no regional fat mass (FM) assessment models have been provided. Hence, we aimed to develop and validate BIA-derived equations to predict regional FM against dual-energy X-ray absorptiometry (DXA) in healthy adults. One hundred and forty-eight adults (77 females) were included in this cross-sectional investigation. DXA assessed whole-body and regional FM, and raw bioelectrical parameters of distinct body regions were measured using a 50 kHz phase-sensitive BIA analyzer. BIA-derived equations were developed for each sex using a stepwise multiple linear regression approach in 2/3 of the sample and cross-validated in the remaining sample. The BIA-derived equations exhibited moderate to very strong relationships ($p < 0.001$) with DXA-measured FM of all body regions in females ($r=0.650$ to 0.907) and males ($r=0.401$ to 0.807). Also, for all the models, no significant deviation from linearity was found ($p>0.10$). Agreement analyses revealed no associations between the differences and the means of the predicted and DXA-derived FM. However, the limits of agreement were large, with individual errors exceeding 50% in females and 70% in males. While the new BIA-derived equations provide a valid estimate of regional FM in middle-aged healthy adults at the population level, demonstrating a cost-effective alternative to DXA for assessing regional FM, caution is advised when applying these equations for individual-level analysis.

Key words: Body composition assessment; bioelectrical impedance analysis; dual-energy X-ray absorptiometry; regional body composition

Abbreviations: Bioelectrical impedance analysis (BIA), body mass index (BMI), coefficient of variation (CV), dual-energy x-ray absorptiometry (DXA), extracellular water (ECW), fat-free mass (FFM), fat mass (FM), intracellular water (ICW), limits of agreement (LOA), pure error (PE), resistance (R), reactance (Xc), impedance (Z), and phase angle (PhA), root mean square error (RMSE).

INTRODUCTION

Body composition assessment is crucial in a variety of physiological and pathological circumstances. Clinical uses include the identification of sarcopenia (1) and excess adiposity, which are responsible for increasing the risk of several chronic diseases (2, 3). Moreover, assessing body composition is valuable for evaluating the impact of specific exercise or nutritional interventions.

While the majority of current research has been on estimating overall body composition, there is limited literature regarding the validity of regional body composition estimates (4). Currently recognized techniques for determining regional body composition include computed tomography, magnetic resonance imaging, and dual-energy x-ray absorptiometry (DXA) (5). However, these technologies can be cost-prohibitive and logistically challenging to access (5). Therefore, developing more accessible methods for estimating regional estimates is crucial. Historically, bioelectrical impedance analysis (BIA) devices provided only whole-body estimates, but advancements have led to tetrapolar BIA analyzers with 8-point electrodes on hands and feet, enabling regional body composition assessment (6). The principles of BIA for body composition assessment have been thoroughly described elsewhere (6, 7).

Choosing appropriate prediction equations is crucial for accurately determining body composition with BIA (8). However, many BIA devices do not disclose the equations used in their software (9). Also, some devices do not display the raw data (i.e., resistance [R], reactance [Xc], impedance [Z], and phase angle [PhA]), restricting the ability to calculate body composition components with a suitable equation (9). This lack of transparent information and data availability hinders accurate and comparable body composition results. Although BIA equations have a lengthy history of development and validation, they have primarily focused on estimating total fat-free mass (FFM) (10). Because a significant portion of FFM corresponds to water (i.e., ~73% hydration fraction), representing an important molecular component influencing multiple biophysical properties (i.e., R, Z, and PhA), there is a strong theoretical rationale sustaining how BIA assessments can provide valuable estimations of FFM. Other studies focused on estimating fat mass (FM) either through indirect calculations (i.e., body mass – FFM) or BIA equation models (10). Although the prediction of BIA-derived FM does not offer a strong theoretical basis as FFM, given that Z and other raw BIA variables are more closely dependent on variables enhancing electrical conductivity (e.g., FFM), there are less direct relationships underlying the prediction of FM that must be considered. For example, due to the presence of specific fat-related components

within the body, including the lipidic composition of cell membranes and organelles, specific interactions can be expected with Xc and capacitance properties, potentially influencing PhA (11). Notwithstanding the specific and independent associations between FM and BIA parameters, which differ from those of FFM, further research is needed to strengthen the empirical foundation of these associations.

Moreover, although the estimation of FFM allows an indirect estimation of FM at the whole-body level (e.g., subtraction of FFM to body mass), the regional analysis benefits from a direct assessment of individual body composition components. This need arises from the current challenge of accurately determining the mass of specific body segments. With the advent of tetrapolar BIA analyzers, evidence has been focusing on developing models predicting FFM and other muscle indicators (e.g., lean soft tissue) at the regional level using whole-body and regional BIA parameters (12). However, there has been limited research developing models estimating regional FM (10), particularly considering that the only available study was conducted in morbidly obese patients (13). Since no regional FM assessment models are currently available for healthy populations, we aimed to develop and validate the first BIA-derived equations to predict regional FM against DXA in healthy adults.

METHODS

Participants

In this cross-sectional study, 148 healthy individuals were included (52.0% of whom were female). Exclusion criteria included skin wounds at the electrode implantation sites, active pregnancy, amputated limbs, implanted medical equipment, orthopedic prostheses, use of medication with impact on water compartments, or the presence of clinical disorders that could affect the water compartments.

The Ethics Committee of the Faculty of Human Kinetics, University of Lisbon (Lisbon, Portugal) approved the study (approval number 12/2020) and it was conducted according to the declaration of Helsinki for human studies from the World Medical Association (14).

Body composition measurements

The literature emphasizes the critical importance of standardized protocols - encompassing dietary intake, physical activity, and participant preparation - in minimizing

errors and enhancing the precision and reliability of body composition measurements obtained through methods such as BIA (8) and DXA (15). Accordingly, all participants' body composition was assessed in standardized environmental and physiological conditions – i.e., assessments conducted between 7 a.m. and 9 a.m., room temperature set at 23ºC, participants with a 12-hour fast, with an empty bladder, and without metal accessories (e.g., rings, earrings, necklaces, and watches). Before participation, participants were asked to maintain regular dietary habits, avoid vigorous exercise sessions for 24 hours before the assessment day, and refrain from smoking for 8 hours.

Anthropometric measurements

Body mass and height were measured to the nearest 0.01 kg and closest 0.1 cm, respectively, on an electronic scale with an integrated stadiometer (SECA 796 Hamburg, Germany). Body mass index (BMI) was calculated as body mass/height^2 (kg/m^2).

Bioelectrical impedance analysis

The impedance measurements were performed using a phase-sensitive single-frequency BIA (BIA 101 BIVA PRO, Akern S.R.L., Florence, Italy), which applies an alternating current of 245 microamperes at 50 kHz. Achieving valid and reproducible measurements through BIA necessitates protocol standardization (8). Following a five-minute rest period to stabilize body fluids, the subjects were placed in a supine position with a leg opening of 45° compared to the median line of the body and the upper limbs positioned 30° away from the trunk. The dorsal surface of both hands and feet was cleaned with isotropic alcohol (70%) and used to place four injecting current electrodes in the plane of the head of the third metacarpal and third metatarsal, respectively. The dorsal surface of both wrists and tibia-tarsal joints was used to place the remaining four electrodes in the middle of an imaginary plane between the two malleoli of each hand and foot, respectively.

Raw BIA parameters obtained by this device included the regional R, Xc, PhA, along with the R index, which was calculated by dividing the square of the full height (cm) by the regional R value and the Xc index, which was calculated dividing the square of the full height (cm) by the regional Xc. Additionally, the contribution of the trunk and extremities to overall conductivity was calculated by comparing the ratios of the R and Xc indices of the trunk (mean R and Xc of the right and left trunk) to the extremities (16). The coefficient of variation (CV) in our laboratory for measuring PhA, recognized as direct measure of a phase-sensitive device, was calculated from two independent samples assessed on separate days

(n=8 and n=7). Under identical fasting, pretest, resting, positioning, and assessment conditions as described, the CV was 2.2% for the first sample (n=8) and 2.8% for the second sample (n=7). Moreover, the CV values for measuring regional PhA of the first and second samples were, respectively, 4.6 and 4.0% for the right arm, 4.5 and 4.4% for the left arm, 4.3 and 4.4% for the right leg, 3.0 and 2.3% for the left leg, 2.0 and 1.7% for the right trunk, and 1.7 and 1.9% for the left trunk.

Dual-energy X-ray absorptiometry (DXA)

Using a DXA fan-beam densitometer (Hologic Explorer-W, fan-beam densitometer, software QDR for Windows version 12.4, Waltham, MA, USA), total and regional FM (kg) were estimated employing a standardized protocol. Daily calibrations were performed by the same laboratory technician and involved scanning a step phantom with six fields of acrylic and aluminium of varying thickness and known absorptive properties to serve as an external standard for analyzing various tissue components. The CV value for measuring total FM, based on two independent samples assessed on separate days, was 0.18% (n=8) and 0.47% (n=7). For regional estimates, the CV values of both samples corresponded, respectively, to 0.56 and 0.81% for the right arm, 0.91 and 0.64% for the left arm, 0.74 and 0.58% for the right leg, 0.66 and 0.39% for the left leg, and 0.70 and 0.89% for the trunk. In both days, the variability measures were taken with the participants under the exact same standardized conditions previously described.

Statistical analysis

IBM SPSS Statistics® (IBM, Chicago, Illinois, USA) version 29.0 for Windows® was used for data analysis. Statistical significance was set at $p < 0.05$ (two-sided). Descriptive characteristics were presented as means, standard deviations, and ranges (minimum-maximum). Normality was assessed using the Kolmogorov–Smirnov test ($n \geq 50$) for the development sample and the Shapiro–Wilk test ($n < 50$) for the validation sample. Differences in the characteristics of development and validation groups were assessed using t-tests (for normally distributed variables) and Mann–Whitney U test (for skewed variables).

The prediction equations were developed using a cross-validation method. A random selection process in Excel chose 100 participants (approximately two-thirds of the sample) for the development group, while the remaining 49 participants (approximately one-third) were used for validation. A sample size of approximately 50 participants per sex provided

sufficient power for the development of sex-specific models and achieved a moderate effect size for the R^2, while considering the inclusion of two independent predictors (i.e., ≥2 participants per predictor rule) (17), a type-1 error of 5% and a power of 80%.

Equation development

A multiple linear regression approach with stepwise selection procedures was used for developing the DXA-derived FM models of specific body regions using the development group. Predictor variables tested included age, side dominance, ethnicity, height, height squared, sitting height, body mass, body mass squared, BMI, inverse BMI (i.e., 1/BMI), and regional raw BIA-derived measures (i.e., Xc, R, PhA) and indexes (i.e., R index, Xc index, R index, Xc index, IndexR_Trunk/Extremities, IndexXc_Trunk/Extremities, and mean R and Xc of the left and right trunk). The variance inflation factor (VIF, threshold of VIF <5) and tolerance analysis (threshold of tolerance >0.20) were employed to assess multicollinearity among independent variables, while diagnostic plot analysis was performed to verify linearity, homoscedasticity, and the normality of residuals. The predicting model with the lowest root mean square error (RMSE) and the highest adjusted R^2 was selected for cross-validation analysis and applied to the validation sample.

Equation cross-validation

The closeness of fit between the BIA-predicted and DXA-measured FM of each segment was assessed by testing the intercept and slope against the null values of 0 and 1. The overall performance of the new developed equations was tested using i) the paired sample t-test, to compare mean values of BIA-predicted and DXA-measured FM; ii) Lin's concordance correlation coefficient test, to verify concordance between BIA-predicted and DXA-measured FM; iii) non-parametric Passing-Bablok regression, to provide an analytical agreement of both predicted and measured FM; iv) pure error (PE), which is the square root of the mean of squares of differences between the DXA measured and predicted FM, was calculated to test the performance of the predictive equations; v) the Bland and Altman analysis (18), to determine the limits of agreement (LOA) (mean difference ±2 SD) between BIA-predicted and DXA-measured FM of all body regions. The statistical significance was set at p-value <0.05.

RESULTS

Tables 1 and 2 present the participants' characteristics and body composition for the development and cross-validation samples. The development sample consisted of 51 females and 49 males, while the cross-validation sample included 26 females and 22 males. No differences were observed for all variables between the groups.

Table 3 shows the developed prediction equations for estimating regional FM. In the regression analysis, for left and right arms and for both sexes, BMI and PhA specific for each segment explained ≃90% (right arm: Adj.R^2 = 0.901, RMSE = 0.203 kg; left arm: Adj.R^2 = 0.923, RMSE = 0.188 kg) for females and ≃70% for males (right arm: Adj.R^2 = 0.700, RMSE = 0.145 kg; left arm: Adj.R^2 = 0.719, RMSE = 0.157 kg) of the variance in FM determined by DXA, respectively.

Regarding females, body mass, height^2, and right leg PhA explained 89% (Adj.R^2 = 0.891, RMSE = 0.758 kg) of the variance in DXA-measured right leg FM, while BMI, height, and IndexXc_Trunk/Extremities explained 84% (Adj.R^2 = 0.843, RMSE = 0.853 kg) of the variance in DXA-measured left leg FM. The mean R of the right and left trunk and BMI explained 93% (Adj.R^2 = 0.929, RMSE = 1.494 kg) of the variance in trunk FM measured through DXA.

Regarding males, body mass^2 and right leg PhA explained 41% (Adj.R^2 = 0.414, RMSE = 0.713 kg) of the variance in DXA-measured right leg FM, while height^2, left leg PhA, and IndexR_Trunk/Extremities explained 52% (Adj.R^2 = 0.517, RMSE = 0.758 kg) of the variance in DXA-measured left leg FM. The mean R of the right and left trunk, BMI, and age explained 78% (Adj.R^2 = 0.781, RMSE = 1.410 kg) of the variance in trunk FM measured through DXA.

Correlations between predictive variables and DXA-derived FM variables, stratified by sex, are presented in Supplementary Tables 1 to 11.

Cross-validation of the developed prediction equations for estimating regional FM

No significant bias, calculated as the mean differences between the prediction equation and the DXA region of interest, was found for all body regions (Table 3). For all the models, using the Passing & Bablock method, no significant deviation from linearity (P>0.10) was found. Figure 1 displays the degree of agreement between BIA-predicted FM of the body regions and that measured by DXA with the line of identity.

Figure 2 depicts the Bland-Altman analyses. Though no trends between the differences and the means of the BIA predicted and DXA-derived FM were observed, LOA were large, representing individual errors that can reach ~50% for females and ~70% for males of the actual DXA regional FM (Table 3).

DISCUSSION

We propose new BIA-derived equations for predicting regional FM in healthy adults. To our knowledge, no other equations in the literature utilize raw BIA parameters to predict regional FM. Our study addresses this gap by providing several validated equations that provide valid estimations for regional FM, offering a viable alternative to DXA, especially for applications involving large-scale populations.

A recent systematic review by Campa et al. (10) identified two equations for total body FM estimation using BIA raw data, one developed for padel players (n=15) (19) and the other for elderly individuals (n=46) (20). In contrast, research on segmental FM estimation is limited, with Jimenez et al. (13) being a notable exception, having developed an equation to estimate DXA-derived trunk FM based on anthropometric and impedance parameters. Notably, while some studies use raw BIA formulas to determine total FM directly, FM is more commonly derived indirectly as the difference between body mass and FFM, which is a more commonly estimated component. However, this indirect approach is not feasible for regional estimates, highlighting the need for specific segmental equations. Our study addresses this gap by extending the application of BIA through the development and validation of equations for segmental FM estimation across all body regions in healthy adults.

Total body FM estimation using BIA raw data is well-documented and provides valuable insights, revealing that inbuilt equations often overestimate or underestimate FM (10). This study extends the application of BIA by developing and validating equations for segmental FM estimation. Previous investigations have compared several BIA devices to DXA for regional body composition assessment, but they relied on the built-in proprietary equations of the devices (21-24). Wingo et al. (24) reported significant discrepancies between an RJL Quantum IV device and DXA in segmental FM estimates in 30 healthy adults. Similarly, Raymon et al. (23) found that the InBody 770 significantly underestimated arm and leg FM compared with DXA in 44 male collegiate athletes. Moore et al. (21), using an RJL Quantum V in 179 adults, reported that while segmental FM estimates were strongly correlated, BIA generally underestimated segmental FM, except for an overestimation of arm FM in females. Contrary to these findings, all FM estimates in our study did not exhibit

significant mean differences in the cross-validation sample. Also, proportional bias was not observed for any FM estimate, unlike Moore et al. (21) and Raymond et al. (23), who reported proportional bias for arms and legs FM.

Although regional Xc would be expected to emerge as a valid predictor of FM, considering the implication of lipidic structures on capacitive properties, only regional PhA stood out as a significant raw BIA predictor in appendicular FM estimation, with lower PhAs predicting higher adiposity values. This finding may not be surprising as previous studies showed significant negative and positive associations between PhA with FM (25) and FFM (26), respectively. Since PhA relies on both Xc and R (i.e., PhA = arctan[(Xc/R) x (180/Π)]), its contribution to predicting regional FM may reflect physiological factors directly involved in the associations between other with raw BIA variables and FM. For instance, FM enlargement is related to an altered distribution of body fluids, specifically a higher extracellular to intracellular water (ECW/ICW) ratio, recognized to be inversely related to PhA (6). In fact, individuals with overweight or obesity may reveal an ECW/ICW ratio > 0.85, i.e., above the average for the normal weight population (~0.70–0.75) (27, 28). This condition is partly proven by the fact that the adipose tissue itself has a higher ECW/ICW ratio than skeletal muscle mass (29). In fact, while FFM has an average ECW/ICW ratio of about 0.80, adipose tissue can achieve a ratio of up to ~ 3.7 (30). Therefore, adiposity is accompanied by a higher extracellular expansion compared to the ICW compartment due to different mechanisms that may include water retention, excess total body water caused by altered hydration regulation, edema (generally present in the lower limbs), hormonal responses related to adipose tissue, insulin resistance, high triglyceride levels, metabolic syndrome, low HDL cholesterol levels, and malnutrition (31, 32). Higher PhA values are observed in athletes, while lower values are seen in sarcopenic obese subjects and individuals with impaired quality of life and poor prognosis in various chronic diseases (33, 34). Still, it is important to highlight that the RI is the most important predictor of fluid-related volumes, i.e., body water and lean mass, accounting for approximately 80-90% of the variance in total and regional lean mass estimations (12, 35, 36). Nevertheless, our regional FM models provided similar wide 95% LOA, aligning with results found for lean mass prediction in athletes (37) and healthy adults (12). While these equations' accuracy is generally sufficient for population-level studies, using more accurate methods remains essential when individual accuracy is crucial. Nonetheless, despite the wide LOA observed in our study, they are narrower than those reported in the literature for the equations integrated into the BIA devices (21, 23). Interestingly, Moore et al. also reported narrower relative LOA in females compared

to males when using the RJL Quantum V manufacturer's software for regional FM estimation against DXA in a sample of 179 adults (21).

While DXA offers regional quantification of body composition and exposes subjects to significantly less radiation than computed tomography scans, its routine clinical use is limited by the high cost of the equipment (5). In contrast, BIA devices are commonly used within general populations due to their quick procedure, minimal required expertise, portability, and cost-effectiveness (38). Furthermore, advances in BIA technology, particularly the development of 8-electrode systems with configurations similar to the traditional 4-electrode setup, but arranged to target different body segments, have significantly enhanced the accuracy of regional body composition estimation (16). This technological approach accounts, for example, for biological variations in body shape, such as differences in body length and trunk-to-extremity proportions, making them a more reliable tool for diverse populations. Therefore, our new equations enable rapid and accurate predictions of regional FM, particularly at the population level, further enhancing the utility of these methods on a large scale.

It is important to highlight the strengths and limitations of the present study. This investigation is the first to develop multiple nonproprietary equations for independently estimating regional FM. While these equations offer a cost-effective and time-efficient alternative to DXA for assessing regional FM in adults with distinct body composition profiles (i.e., normal weight, overweight, and obese), it is important to acknowledge that the rationale supporting the relationship between FM and the predictive variables, particularly those related to BIA assessment, is less robust than that observed with FFM, requiring further investigation. Despite the underlying mechanisms explaining FM not being fully understood, the developed models were grounded on physiological principles rather than merely capturing spurious correlations or population-specific patterns, which enhances the generalizability of our prediction equations. Another limitation was the use of DXA as the reference method for developing the prediction equations. However, while magnetic resonance imaging and computed tomography are recognized as more precise measures of regional body composition, they are cost-prohibitive, logistically challenging to access, and require highly trained technicians (5). There is also the barrier of high exposure to ionizing radiation with computed tomography (5).

In conclusion, the developed BIA-derived equations provide a valid estimate of regional FM in healthy adults, demonstrating a cost-effective alternative to DXA. More specifically, the new equations can be regarded as a tool for large-scale application with

valuable insights into population health and specific risks related to FM distribution – e.g., identifying regional adiposity patterns at the population level and determining how regional FM impacts mobility and physical function. Nevertheless, caution is advised when using BIA for individual regional FM analysis. Future research should aim to validate these equations in diverse populations and investigate their ability to reliably track changes in regional FM over time, ensuring broader applicability and robustness.

ACKNOWLEDGEMENTS

The authors express their gratitude to all the participants involved in this study.

AUTHORS' CONTRIBUTIONS

AMS and LBS conceived and planned the experiments. GBR, JPM, PBJ, and IRC carried out the experiments and data collection. AMS, TRS, MHR, PBJ and AB did the data analysis. AMS and TRS took the lead in writing the manuscript. All authors provided critical feedback and helped shape the research, analysis, and manuscript.

FINANCIAL SUPPORT

This investigation was conducted at the Interdisciplinary Center of the Study of Human Performance (CIPER), Faculdade de Motricidade Humana, Universidade de Lisboa, and supported by fellowships from the Portuguese Foundation for Science and Technology (grant to GBR: 2020.07856.BD; grant to IRC: SFRH/BD/149394/2019; grant within the unit I&D 472 -UIDB/00447/2020).

CONFLICTS OF INTEREST

The authors declare that they have no conflict of interest.

REFERENCES

1. Cruz-Jentoft AJ, Bahat G, Bauer J, Boirie Y, Bruyère O, Cederholm T, et al. Sarcopenia: revised European consensus on definition and diagnosis. Age Ageing. 2019;48(1):16-31.

2. Vazquez G, Duval S, Jacobs DR, Jr., Silventoinen K. Comparison of body mass index, waist circumference, and waist/hip ratio in predicting incident diabetes: a meta-analysis. Epidemiol Rev. 2007;29:115-28.

3. Wormser D, Kaptoge S, Di Angelantonio E, Wood AM, Pennells L, Thompson A, et al. Separate and combined associations of body-mass index and abdominal adiposity with cardiovascular disease: collaborative analysis of 58 prospective studies. Lancet. 2011;377(9771):1085-95.

4. Fosbøl M, Zerahn B. Contemporary methods of body composition measurement. Clin Physiol Funct Imaging. 2015;35(2):81-97.

5. Ackland TR, Lohman TG, Sundgot-Borgen J, Maughan RJ, Meyer NL, Stewart AD, et al. Current status of body composition assessment in sport: review and position statement on behalf of the ad hoc research working group on body composition health and performance, under the auspices of the I.O.C. Medical Commission. Sports Med. 2012;42(3):227-49.

6. Kyle UG, Bosaeus I, De Lorenzo AD, Deurenberg P, Elia M, Gómez JM, et al. Bioelectrical impedance analysis-part I: review of principles and methods. Clin Nutr. 2004;23(5):1226-43.

7. Lukaski HC. Evolution of bioimpedance: a circuitous journey from estimation of physiological function to assessment of body composition and a return to clinical research. Eur J Clin Nutr. 2013;67 Suppl 1:S2-9.

8. Kyle UG, Bosaeus I, De Lorenzo AD, Deurenberg P, Elia M, Manuel Gómez J, et al. Bioelectrical impedance analysis-part II: utilization in clinical practice. Clin Nutr. 2004;23(6):1430-53.

9. Mulasi U, Kuchnia AJ, Cole AJ, Earthman CP. Bioimpedance at the bedside: current applications, limitations, and opportunities. Nutr Clin Pract. 2015;30(2):180-93.

10. Campa F, Coratella G, Cerullo G, Noriega Z, Francisco R, Charrier D, et al. High-standard predictive equations for estimating body composition using bioelectrical impedance analysis: a systematic review. J Transl Med. 2024;22(1):515.

11. Ohki S. The electrical capacitance of phospholipid membranes. Biophys J. 1969;9(10):1195-205.

12. Sardinha LB, Rosa GB, Hetherington-Rauth M, Correia IR, Magalhães JP, Silva AM, et al. Development and validation of bioelectrical impedance prediction equations estimating regional lean soft tissue mass in middle-aged adults. Eur J Clin Nutr. 2023;77(2):202-11.

13. Jiménez A, Omaña W, Flores L, Coves MJ, Bellido D, Perea V, et al. Prediction of whole-body and segmental body composition by bioelectrical impedance in morbidly obese subjects. Obes Surg. 2012;22(4):587-93.

14. World Medical Association Declaration of Helsinki: ethical principles for medical research involving human subjects. Jama. 2013;310(20):2191-4.

15. Hangartner TN, Warner S, Braillon P, Jankowski L, Shepherd J. The Official Positions of the International Society for Clinical Densitometry: acquisition of dual-energy X-ray absorptiometry body composition and considerations regarding analysis and repeatability of measures. J Clin Densitom. 2013;16(4):520-36.

16. Bosy-Westphal A, Schautz B, Later W, Kehayias JJ, Gallagher D, Müller MJ. What makes a BIA equation unique? Validity of eight-electrode multifrequency BIA to estimate body composition in a healthy adult population. Eur J Clin Nutr. 2013;67 Suppl 1:S14-21.

17. Austin PC, Steyerberg EW. The number of subjects per variable required in linear regression analyses. J Clin Epidemiol. 2015;68(6):627-36.

18. Bland JM, Altman DG. Statistical methods for assessing agreement between two methods of clinical measurement. Lancet. 1986;1(8476):307-10.

19. Mauro M, Toselli S, De Giorgi S, Heinrich KM, Di Gioia G, Moretti B, et al. New regression models to predict fat mass in intermediate-level male padel players. Heliyon. 2023;9(8):e18719.

20. Svendsen OL, Haarbo J, Heitmann BL, Gotfredsen A, Christiansen C. Measurement of body fat in elderly subjects by dual-energy x-ray absorptiometry, bioelectrical impedance, and anthropometry. Am J Clin Nutr. 1991;53(5):1117-23.

21. Moore ML, Benavides ML, Dellinger JR, Adamson BT, Tinsley GM. Segmental body composition evaluation by bioelectrical impedance analysis and dual-energy X-ray absorptiometry: Quantifying agreement between methods. Clin Nutr. 2020;39(9):2802-10.

22. Ling CH, de Craen AJ, Slagboom PE, Gunn DA, Stokkel MP, Westendorp RG, et al. Accuracy of direct segmental multi-frequency bioimpedance analysis in the assessment of total body and segmental body composition in middle-aged adult population. Clin Nutr. 2011;30(5):610-5.

23. Raymond CJ, Dengel DR, Bosch TA. Total and Segmental Body Composition Examination in Collegiate Football Players Using Multifrequency Bioelectrical Impedance Analysis and Dual X-ray Absorptiometry. J Strength Cond Res. 2018;32(3):772-82.

24. Wingo BC, Barry VG, Ellis AC, Gower BA. Comparison of segmental body composition estimated by bioelectrical impedance analysis and dual-energy X-ray absorptiometry. Clin Nutr ESPEN. 2018;28:141-7.

25. Streb AR, Hansen F, Gabiatti MP, Tozetto WR, Del Duca GF. Phase angle associated with different indicators of health-related physical fitness in adults with obesity. Physiol Behav. 2020;225:113104.

26. Gonzalez MC, Barbosa-Silva TG, Bielemann RM, Gallagher D, Heymsfield SB. Phase angle and its determinants in healthy subjects: influence of body composition. Am J Clin Nutr. 2016;103(3):712-6.

27. Fogelholm GM, Kukkonen-Harjula TK, Sievänen HT, Oja P, Vuori IM. Body composition assessment in lean and normal-weight young women. Br J Nutr. 1996;75(6):793-802.

28. Fogelholm GM, Sievänen HT, van Marken Lichtenbelt WD, Westerterp KR. Assessment of fat-mass loss during weight reduction in obese women. Metabolism. 1997;46(8):968-75.

29. Cancello R, Brunani A, Brenna E, Soranna D, Bertoli S, Zambon A, et al. Phase angle (PhA) in overweight and obesity: evidence of applicability from diagnosis to weight changes in obesity treatment. Rev Endocr Metab Disord. 2023;24(3):451-64.

30. Wang J, Pierson RN, Jr. Disparate hydration of adipose and lean tissue require a new model for body water distribution in man. J Nutr. 1976;106(12):1687-93.

31. Mazariegos M, Kral JG, Wang J, Waki M, Heymsfield SB, Pierson RN, Jr., et al. Body composition and surgical treatment of obesity. Effects of weight loss on fluid distribution. Ann Surg. 1992;216(1):69-73.

32. Dittmar M, Reber H, Kahaly GJ. Bioimpedance phase angle indicates catabolism in Type 2 diabetes. Diabet Med. 2015;32(9):1177-85.

33. de Blasio F, Santaniello MG, de Blasio F, Mazzarella G, Bianco A, Lionetti L, et al. Raw BIA variables are predictors of muscle strength in patients with chronic obstructive pulmonary disease. Eur J Clin Nutr. 2017;71(11):1336-40.

34. Norman K, Stobäus N, Pirlich M, Bosy-Westphal A. Bioelectrical phase angle and impedance vector analysis--clinical relevance and applicability of impedance parameters. Clin Nutr. 2012;31(6):854-61.

35. De Rui M, Veronese N, Bolzetta F, Berton L, Carraro S, Bano G, et al. Validation of bioelectrical impedance analysis for estimating limb lean mass in free-living Caucasian elderly people. Clin Nutr. 2017;36(2):577-84.

36. Toselli S, Campa F, Matias CN, de Alencar Silva BS, Dos Santos VR, Maietta Latessa P, et al. Predictive equation for assessing appendicular lean soft tissue mass using bioelectric impedance analysis in older adults: Effect of body fat distribution. Exp Gerontol. 2021;150:111393.

37. Sardinha LB, Correia IR, Magalhães JP, Júdice PB, Silva AM, Hetherington-Rauth M. Development and validation of BIA prediction equations of upper and lower limb lean soft tissue in athletes. Eur J Clin Nutr. 2020;74(12):1646-52.

38. Kasper AM, Langan-Evans C, Hudson JF, Brownlee TE, Harper LD, Naughton RJ, et al. Come Back Skinfolds, All Is Forgiven: A Narrative Review of the Efficacy of Common Body Composition Methods in Applied Sports Practice. Nutrients. 2021;13(4).

Table 1 Characteristics of the development group (n=100).

	Total (n=100)		Female (n=51)		Male (n=49)	
	Mean	SD	Mean	SD	Mean	SD
Age (years)	31.5	11.2	34.7	11.6	28.3	10
Body mass (kg)	69.7	14.1	65.4	16.8	74.2	8.8
Height (cm)	168.2	9.2	161.3	6.5	175.4	5.3
BMI (kg/m^2)	24.6	4.3	25.1	5.5	24.1	2.6
FM (kg)	17.7	9.4	21.5	11.1	13.7	4.9
FM (%)	25.4	10	31.9	8.9	18.6	5.6
FFM (kg)	51.1	10.9	43	70.8	59.4	7.1
Right Arm FM (kg)	0.9	0.5	1.1	0.6	0.6	0.3
Left Arm FM (kg)	0.9	0.6	1.2	0.7	0.7	0.3
Right Leg FM (kg)	3.5	2	4.5	2.3	2.5	0.9
Left Leg FM (kg)	3.5	1.9	4.4	2.2	2.4	0.9
Trunk FM (kg)	8.1	4.7	9.5	5.6	6.5	2.9
Right Arm R (Ω)	260	49.1	293.2	39.5	225.4	31
Right Arm Xc (Ω)	26.6	3.2	27.2	3.3	25.9	3
Right Arm PhA (º)	6	0.9	5.3	0.5	6.6	0.7
Left Arm R (Ω)	269.4	49.7	303	39.6	234.4	31.7
Left Arm Xc (Ω)	26.1	3	26.6	3.1	25.6	2.8
Left Arm PhA (º)	5.7	0.9	5.1	0.6	6.3	0.6
Right Leg R (Ω)	238.9	32.8	251.4	32.3	225.8	28
Right Leg Xc (Ω)	28.8	4	28.6	4.4	29.1	3.4
Right Leg PhA (º)	6.9	0.8	6.5	0.7	7.4	0.7
Left Leg R (Ω)	246.2	37.1	259	39.5	232.8	29.3
Left Leg Xc (Ω)	28.7	4	28.3	4.3	29.2	3.7
Left Leg PhA (º)	6.7	0.8	6.3	0.7	7.2	0.7
Left and Right Trunk R (Ω)	21	3.3	22.9	2.7	19	2.6
Left and Right Trunk Xc (Ω)	15.2	2.8	15.9	1.4	14.4	3.6
Left and Right Trunk PhA (º)	35.8	7.1	34.9	4.5	36.7	9.1

Abbreviations: **BMI** body mass index, **FFM** fat-free mass, **FM** fat mass, **PhA** phase angle, **R** resistance, **Xc** reactance.

Table 2 Characteristics of the validation group (n=48).

	Total (n=48)		Female (n=26)		Male (n=22)	
	Mean	SD	Mean	SD	Mean	SD
Age (years)	33.1	13.9	32.4	12.3	34.0	15.9
Body mass (kg)	74.1	16.5	69.3	15.3	79.7	16.4
Height (cm)	169	9.7	163.5	7.5	175.5	7.9
BMI (kg/m^2)	25.9	5.2	25.9	5.8	25.8	4.5
FM (kg)	19.6	9.8	22.0	11.2	16.8	7.3
FM (%)	26.4	9.7	31.0	9.9	20.9	5.8
FFM (kg)	53.3	12.4	46.4	86.2	61.5	11.3
Right Arm FM (kg)	0.9	0.6	1.1	0.7	0.8	0.4
Left Arm FM (kg)	1.0	0.6	1.2	0.7	0.8	0.4
Right Leg FM (kg)	3.7	1.9	4.6	2.1	2.7	1.1
Left Leg FM (kg)	3.7	1.9	4.6	2.0	2.7	1.0
Trunk FM (kg)	9.3	5.5	9.6	6.0	8.8	5.0
Right Arm R (Ω)	260.3	50.0	283.3	43.3	233.1	44.1
Right Arm Xc (Ω)	26.7	3.4	27.3	3.4	26.1	3.4
Right Arm PhA (º)	6.0	0.9	5.6	0.8	6.5	0.9
Left Arm R (Ω)	272.4	50.4	293.4	45.4	247.6	45.2
Left Arm Xc (Ω)	26.4	3.2	26.8	3.5	26.0	2.8
Left Arm PhA (º)	5.7	0.9	5.3	0.7	6.1	0.8
Right Leg R (Ω)	238.7	35.5	245.8	37.1	230.3	32.3
Right Leg Xc (Ω)	29.1	4.5	29.0	4.9	29.2	4.2
Right Leg PhA (º)	7.0	0.8	6.8	0.7	7.3	0.8
Left Leg R (Ω)	243.4	37.5	249.5	40.7	236.1	32.8
Left Leg Xc (Ω)	28.8	4.3	28.4	4.5	29.3	4.1
Left Leg PhA (º)	6.8	0.8	6.5	0.7	7.1	0.8
Left and Right Trunk R (Ω)	20.3	3.4	21.1	3.2	19.4	3.5
Left and Right Trunk Xc (Ω)	15.4	1.8	15.5	0.4	15.3	2.7
Left and Right Trunk PhA (º)	37.6	6.9	36.7	4.5	38.6	9.0

Abbreviations: **BMI** body mass index, **FFM** fat-free mass, **FM** fat mass, **PhA** phase angle, **R** resistance,

Xc reactance.

Table 3 Developed prediction equations using development group (n=100) for estimating DXA-derived FM from BIA and performance analysis of developed prediction equations using the cross-validation group (n=48).

	Development (n=100)[†]				**Cross-validation (n=48)**[¥]						
	Equation[±]	**r**	**Adj. R^2**	**RMSE**	**Adj. R^2**	**PE**	**Bias***	**LOA**	**LOA (%)**	**Trend (r)**[#]	**CCC**
	Females	(n=51)			(n=26)						
Right arm (kg)	-0.988 + 0.112*BMI – 0.137*Right Arm PhA	0.951	0.901	0.203	0.904	0.223	-0.054	-0.50; 0.39	-46%; 36%	0.322	0.944
Left arm (kg)	-0.828 + 0.119*BMI – 0.195*Left Arm PhA	0.962	0.923	0.188	0.907	0.213	-0.047	-0.47; 0.37	-40%; 31%	0.075	0.952
Right leg (kg)	3.481+0.132*Body Mass - 0,00017*Height^2 -0.474*Right Leg PhA	0.947	0.891	0.758	0.737	1.048	-0.245	-2.40; 1.90	-52%; 41%	0.022	0.858
Left leg (kg)	-11,214 + 0.409*BMI + 0.05*Height - 4.478* IndexXc_Trunk/Extremities	0.923	0.843	0.853	0.650	1.151	-0.430	-2.80; 2.00	-61%; 44%	-0.050	0.795
Trunk (kg)	-24.360+ 1.027*BMI +0.355* Mean Left and Right Trunk R	0.965	0.929	1.494	0.884	2.010	-0.161	-4.20; 3.90	-44%; 41%	-0.028	0.942
	Males	(n=49)			(n=22)						
Right arm (kg)	-0.005 + 0.078*BMI – 0.185*Right Arm PhA	0.843	0.700	0.145	0.796	0.161	-0.044	-0.35; 0.27	-46%; 35%	0.114	0.897
Left arm (kg)	0.046 + 0.090*BMI -0.242*Left Arm PhA	0.856	0.719	0.157	0.807	0.152	-0.090	-0.43; 0.25	-53%; 31%	-0.220	0.862

Right leg (kg)	5.354+0.000396*Body Mass^2- 0.694*Right Leg PhA	0.664	0.414	0.713	0.401	0.793	-0.282	-2.20; 1.64	-83%; 62%	-0.236	0.626
Left leg (kg)	2.526+0.00039*Body Mass^2 -0.564*Left Leg PhA + 21.588* IndexR_Trunk/Extremities	0.733	0.517	0.758	0.440	0.766	-0.196	-2.03; 1.63	-76%; 61%	-0.248	0.662
Trunk (kg)	-25.706+0.845*BMI +0.519* Mean Left and Right Trunk R + 0.067*Age	0.892	0.781	1.410	0.878	1.720	0.351	-3.10; 3.80	-35%; 43%	0.374	0.929

Abbreviations**: Adj.R^2** adjusted coefficient of determination, **RMSE** root mean square error, **PE** pure error, **LOA** limits of agreement at 95% confidence interval, **CCC** Lin's concordance correlation coefficient, **FM** fat mass, **BMI** body mass index, **PhA** Phase angle (º), **IndexR_Trunk/Extremities** resistance index of the ratio between trunk to extremities, **IndexXc_Trunk/Extremities** reactance index of the ratio between trunk to extremities.

† Passing & Bablock method did not show models deviating from linearity (p>0.10);

¥ regression lines did not differ from the line of identity (i.e., slope and intercept did not differ from 1 and 0, respectively);

± R^2 changed significantly (p<0.05); no multicollinearity was observed (VIF<5 and Tolerance>0.20);

* bias, calculated as the mean differences between the DXA region of interest and the new equation;

association between the differences and the mean of the methods.

Figure 1 Relationship between DXA measured FM and BIA predicted FM for a) right arm, b) left arm, c) right leg, d) left leg, and e) trunk. Regression lines of females (empty circles) and males (filled circles) are represented as dashed and solid lines (black), respectively. Lines of identity are represented as solid lines (gray).

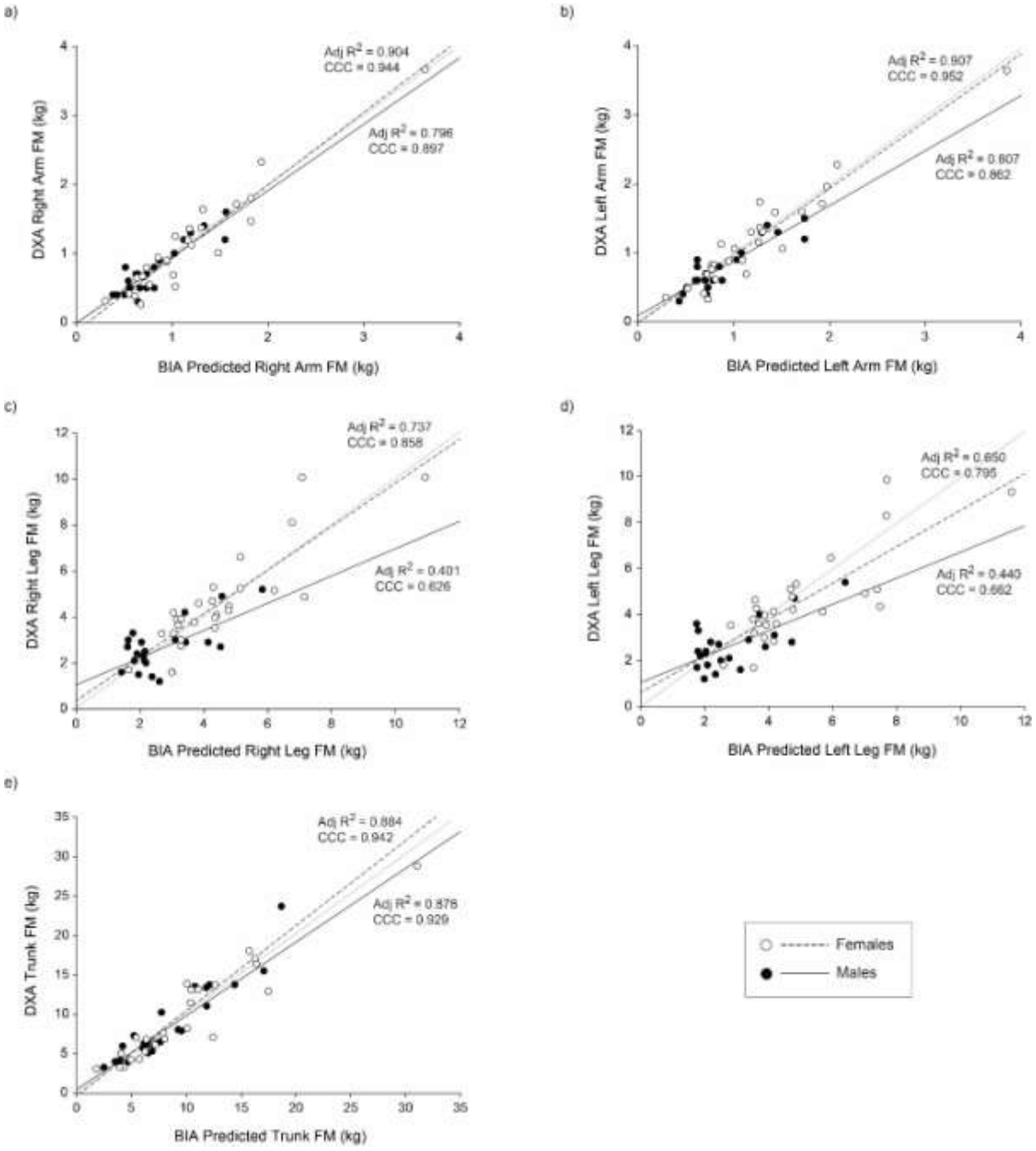

Figure 2 Bland–Altman plot of the difference between DXA measured FM and BIA predicted FM with the average DXA measured FM and BIA predicted FM for a) right arm, b) left arm, c) right leg, d) left leg, and e) trunk. 95% limits of agreement (LOA) of females (empty circles) and males (filled circles) are represented as dashed and solid lines (black), respectively.